International Journal of
Molecular Sciences

MDPI

Article

Carboxamide Derivatives Are Potential Therapeutic AHR Ligands for Restoring IL-4 Mediated Repression of Epidermal Differentiation Proteins

Gijs Rikken [1], Noa J. M. van den Brink [1], Ivonne M. J. J. van Vlijmen-Willems [1], Piet E. J. van Erp [1], Lars Pettersson [2], Jos P. H. Smits [1,†] and Ellen H. van den Bogaard [1,*,†]

[1] Department of Dermatology, Radboud Institute for Molecular Life Sciences (RIMLS), Radboud University Nijmegen Medical Center (Radboudumc), 6525 GA Nijmegen, The Netherlands; gijs.rikken@radboudumc.nl (G.R.); noa.vandenbrink@radboudumc.nl (N.J.M.v.d.B.); ivonne.vanvlijmen-willems@radboudumc.nl (I.M.J.J.v.V.-W.); piet.vanerp@radboudumc.nl (P.E.J.v.E.); jos.ph.smits@radboudumc.nl (J.P.H.S.)
[2] Immunahr AB, Prästasvängen 21, 224 80 Lund, Sweden; larspettersson59@live.se
* Correspondence: ellen.vandenbogaard@radboudumc.nl; Tel.: +31-24-3614093
† These authors contributed equally to this work.

Abstract: Atopic dermatitis (AD) is a common T-helper 2 (Th2) lymphocyte-mediated chronic inflammatory skin disease characterized by disturbed epidermal differentiation (e.g., *filaggrin* (*FLG*) expression) and diminished skin barrier function. Therapeutics targeting the aryl hydrocarbon receptor (AHR), such as coal tar and tapinarof, are effective in AD, yet new receptor ligands with improved potency or bioavailability are in demand to expand the AHR-targeting therapeutic arsenal. We found that carboxamide derivatives from laquinimod, tasquinimod, and roquinimex can activate AHR signaling at low nanomolar concentrations. Tasquinimod derivative (IMA-06504) and its prodrug (IMA-07101) provided full agonist activity and were most effective to induce *FLG* and other epidermal differentiation proteins, and counteracted IL-4 mediated repression of terminal differentiation. Partial agonist activity by other derivatives was less efficacious. The previously reported beneficial safety profile of these novel small molecules, and the herein reported therapeutic potential of specific carboxamide derivatives, provides a solid rationale for further preclinical assertation.

Keywords: aryl hydrocarbon receptor; carboxamide-3-quinoline; *filaggrin*; drug development; atopic dermatitis

Citation: Rikken, G.; van den Brink, N.J.M.; van Vlijmen-Willems, I.M.J.J.; van Erp, P.E.J.; Pettersson, L.; Smits, J.P.H.; van den Bogaard, E.H. Carboxamide Derivatives Are Potential Therapeutic AHR Ligands for Restoring IL-4 Mediated Repression of Epidermal Differentiation Proteins. *Int. J. Mol. Sci.* **2022**, *23*, 1773. https://doi.org/10.3390/ijms23031773

Academic Editor: Genji Imokawa

Received: 10 December 2021
Accepted: 29 January 2022
Published: 4 February 2022

1. Introduction

During epidermal differentiation, multiple structural proteins are expressed in the last living cell layer, the *stratum granulosum*. Amongst others, filament aggregating protein (*filaggrin*), encoded by the *FLG* gene, is processed into the cornified envelope, an insoluble network consisting of the debris of keratinocytes—corneocytes—that are tightly crosslinked and imbedded in a matrix of lipid components ultimately forming the physical barrier of the skin: the *stratum corneum*. Disturbed epidermal differentiation and skin barrier function loss are key hallmarks of common chronic inflammatory skin diseases such as atopic dermatitis (AD) and psoriasis (Pso). The epidermal differentiation process is affected by the disease-specific cytokine milieu (the Th2-cytokines in AD (e.g., IL-4) or the Th1/Th17 cytokines in Pso), or due to genetic predisposition mostly associated to AD (e.g., *FLG* loss-of-function mutations [1,2], *FLG* copy number variation [3], *hornerin* (*HRNR*)-Single-Nucleotide Polymorphism (SNP) [4,5], *small proline-rich protein 3* (*SPRR3*) [6]. Most therapeutic strategies are aimed at general or targeted immunosuppression combined with indifferent skin moisturizing emollients. However, the direct targeting of the epidermal differentiation process in combination with immunomodulatory effects could be an attractive therapeutic avenue by killing two birds with one stone.

Evidence for such effective therapeutics came from our studies on the molecular mechanism of coal tar. Coal tar is a viscous liquid that is obtained by burning coal and is thought to consist of at least 10,000 chemicals of which many are characterized as polycyclic aromatic hydrocarbons (PAHs). Although topical application of coal tar is an ancient treatment option for AD and Pso, its exact therapeutic mechanism of action has long been unknown, until recently. PAHs in coal tar activate the aryl hydrocarbon receptor (AHR) in keratinocytes, thereby counteracting the keratinocyte activation towards AD-related interleukins and restoring the expression levels of affected differentiation proteins, including that of *FLG* [7]. In addition, genes encoding antimicrobial peptides are upregulated which together with restored differentiation capability and reconstituted skin barrier properties are thought to contribute to dampening of the inflammatory processes in skin [8].

The AHR is a highly conserved receptor and member of the family of basic helix–loop–helix transcription factors, that can be activated by a wide variety of both exogenous and endogenous ligands. Dioxins are a group of chemicals that are considered organic pollutants. TCDD (2,3,7,8-tetrachlorodibenzo-p-dioxin), one of the most widely used polychlorinated dioxins and considered an AHR model ligand, is often used to study AHR signaling in epidermal keratinocytes [9,10]. As TCDD is highly toxic with prolonged half-life of several years, dioxins such as TCDD are not suited for therapeutic purposes. Short-lived AHR ligands include UV-induced endogenous tryptophan metabolites [11] (hence the postulated role for AHR-mediated therapeutic effects of UV therapy in PSo). Other metabolites can be formed by members of the skin's microbiome, and dietary plant constituents, as well as several pharmaceutics [12–15]. Upon activation, AHR signaling is known to regulate a plethora of cellular processes, e.g., embryonic development [16], keratinocyte proliferation and differentiation [17], epidermal barrier formation [14,18], immune cell development [19], angiogenesis [20], and many more [16,18,19,21–24]. However, studies also report contradicting outcomes depending on the tissue and disease context [25], and AHR ligand promiscuity has long been a subject of research [26].

Ever since the working mechanism of coal tar via AHR was elucidated, a search for novel AHR targeting therapeutics has been ongoing. This has led to the development of tapinarof, a natural AHR ligand that is currently in Phase 3 trials as a topical drug for AD and PSo [27,28]. However, other immunomodulatory molecules that are investigated in clinical trials for different indications, such as quinoline-3-carboxamide derivatives, also act on the AHR signaling pathway [29]. Laquinimod (LAQ) targets the AHR and is effective in alleviating disease symptoms in experimental models of multiple sclerosis and Huntington's disease [30] and reduces IL-17 levels [31,32]. Roquinimex (ROQ, the first clinical compound in the series) and tasquinimod (TASQ) have been investigated being potential immunomodulating drugs effective in cancer treatment and in autoimmune diseases. Interestingly, ROQ was found effective against Pso in two patients that were included in a phase 2 clinical renal cell carcinoma trial [33]. Although LAQ, TASQ and ROQ may lead to AHR activation, they do not activate AHR signaling in their original form. Instead, intracellular metabolism generates potent N-dealkylated metabolites that are capable of AHR binding, as previously described in the patent application [34]. These N-dealkylated compounds have been tested in toxicity studies in vitro [35] and as diacetyl prodrugs in vivo [36] at high doses with minor signs of adverse effects. Albeit the structural similarity to TCDD and shared theoretical receptor binding modes [35], these carboxamide derivatives are considered less metabolically resistant as compared to TCDD. The pharmacokinetic clearance of AHR ligands would be important to mitigate the adverse effects of sustained AHR signaling.

In this study, carboxamide derivatives from LAQ, TASQ and ROQ were analyzed for their AHR activating potential in human keratinocytes and in human epidermal models. Primary read out was the expression level of epidermal differentiation genes and proteins. In addition, the ability to rescue deprived *FLG* expression, and other important epidermal

barrier proteins in AD-like organotypic skin models, was investigated to identify new drug candidates for further preclinical testing.

2. Results

2.1. Structure of IMA-Compounds

LAQ and TASQ are both metabolized by CYP3A4 (N-dealkylation) to form the AHR-active metabolites IMA-06201 and IMA-06504 in low concentrations (Figure 1A,B, Supplemental Table S1). These AHR-active compounds have extremely low aqueous solubility and are therefore not appropriate for in vivo or clinical use. Even though prodrugs IMA-08401 and IMA-07101 also have low aqueous solubility, they can easily be formulated (e.g., PEG-400) [36]. Furthermore, the in vivo hydrolysis of the prodrug IMA-08401 results in higher levels of IMA-06201 than corresponding levels from LAQ metabolism (unpublished). Analogously to IMA-06201 and IMA-06504, compound IMA-05101 is an AHR agonist and a metabolite of the clinical compound ROQ. IMA-01403 was synthesized by blocking the IMA-05101 4-OH with a benzyl group, which adds extra bulk and disrupts internal hydrogen bonding, expected to severely reduce the activity of the compound (Figure 1C, Supplemental Table S1).

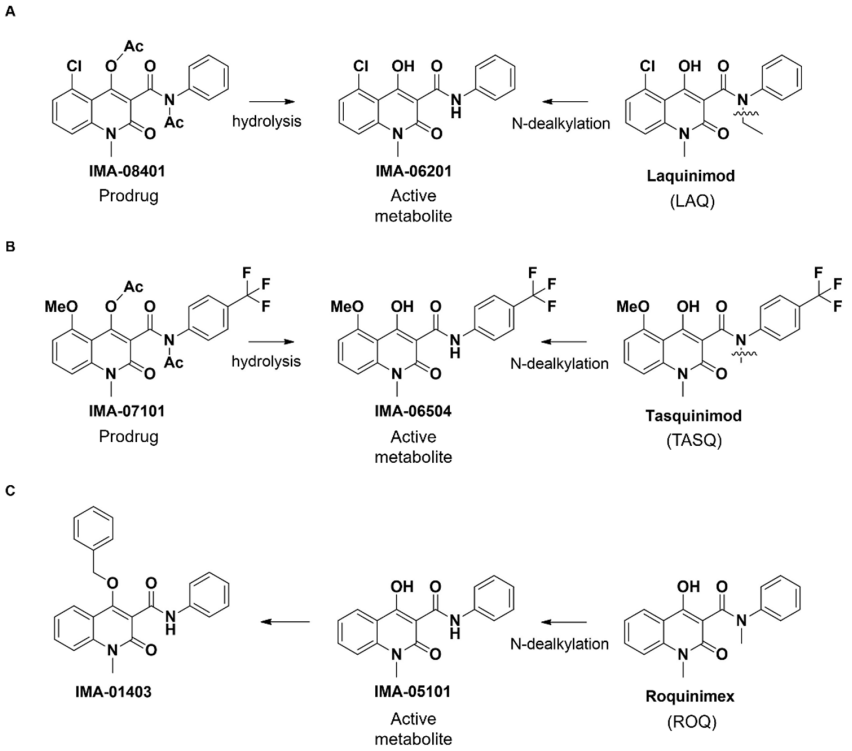

Figure 1. Structure of IMA-compounds. (**A**) Laquinimod (LAQ) is metabolized (N-dealkylation) to form the AHR-active metabolite IMA-06201. Hydrolysis of the prodrug IMA-08401 also forms the IMA-06201 derivative. (**B**) Tasquinimod (TASQ), its AHR-active metabolite IMA-06504, and the prodrug IMA-07101. (**C**) Roquinimex (ROQ), its AHR-active metabolite IMA-05101, and the 4-O-benzyl derivative IMA-01403.

2.2. IMA-Compounds Induce AHR Activity in Reporter Cell Line and Primary Keratinocytes

First, all newly synthesized derivatives were screened for AHR activating potential using the established human HepG2 (40/6) reporter cell line [37]. LAQ was used for comparison being a parent compound, 2,3,7,8-Tetrachlorodibenzo-p-Dioxin (TCDD) was included as a full AHR agonist at a saturating dose of 10 nM. All metabolites and prodrugs derived from LAQ, TASQ, and ROQ were able to activate AHR signaling in a clear dose dependent manner, maximally leading to 110–145% of the TCDD response. Blocking the -OH group in IMA-01403 indeed reduced the agonist activity (Figure 2A).

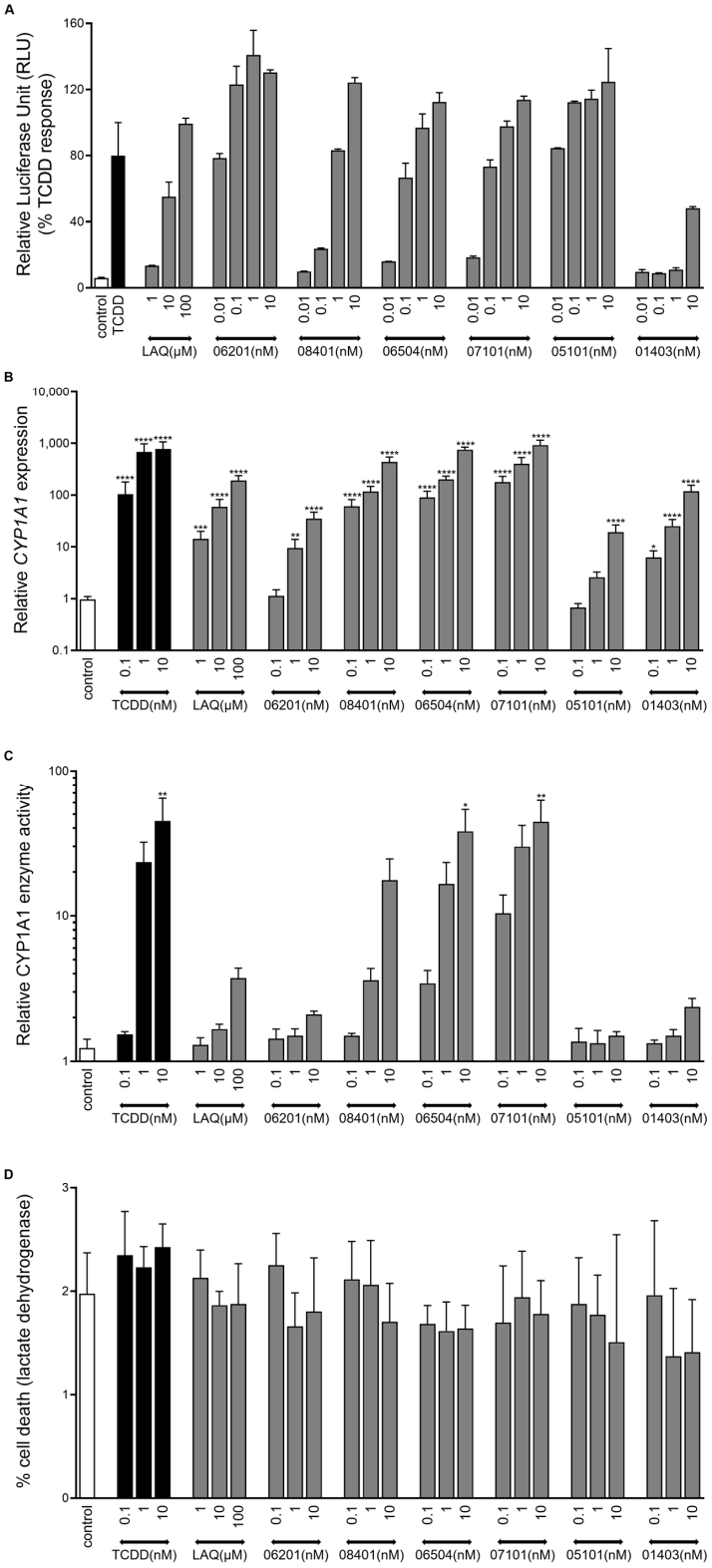

Figure 2. Induction of AHR activity by IMA-derivatives. (**A**) HepG2 40/6 cell cultures stimulated for 4 h with a concentration series of LAQ and IMA-compounds. TCDD (10 nM) was used as a full AHR agonist and set at 100% luminescent activity (n = 2). (**B**) *CYP1A1* mRNA expression levels, (**C**) *CYP1A1* enzyme activity (luminescent assay), and (**D**) percentage cell death (24 h measurement, lactate dehydrogenase (LDH) assay) of primary human keratinocytes (n = 3) stimulated for 48 h (re-stimulated after 24 h) with a concentration series of the IMA-compounds, LAQ, and TCDD. * $p < 0.05$, ** $p < 0.01$, *** $p < 0.001$, **** $p < 0.0001$. Mean +/− SEM.

Next, we subjected primary human keratinocyte monolayer cultures to all derivatives. Again, clear dose dependent gene expression levels of AHR target genes, cytochrome P450 1A1 (*CYP1A1*) and 1B1 (*CYP1B1*) were observed (Figure 2B, Supplemental Figure S1A). Prodrug IMA-07101 and its active metabolite IMA-06504 (from TASQ) and prodrug IMA-08401 (from LAQ) exhibited saturated responses such as those seen after TCDD exposure. *AHRR* gene expression levels indicate the activation of a negative control feedback loop to downscale prolonged AHR activation, which was most evident for TCDD and the TASQ derivatives (Supplemental Figure S1B). Only *CYP1A1* mRNA expression levels reaching a 1000-fold change resulted in significantly induced enzymatic *CYP1A1* activity, as observed for TCDD, IMA-06504, and IMA-07101 (all at 10 nM) (Figure 2C). Cell viability was unaffected in all cell cultures as lactate dehydrogenase (LDH) levels were comparable to control (unstimulated) keratinocyte cultures (Figure 2D).

2.3. AHR-Mediated Expression of Epidermal Differentiation

Given the stimulating effects of coal tar, TCDD, and other AHR ligands on epidermal differentiation through AHR-dependent mechanisms [7,10,38,39], we analyzed the following marker levels for terminal differentiation: *filaggrin* (*FLG*), *hornerin* (*HRNR*), *involucrin* (*IVL*), and *loricrin* (*LOR*) (Figure 3). Stimulation with IMA-07101 significantly and dose-dependently induced *FLG*, *HRNR*, and *IVL* levels, similar to TCDD. Based on these results, we subjected organotypic human epidermal equivalents (HEEs) to 1 nM IMA exposure during the final 96 h of the air–liquid interface culture. In particular, the increase in numbers of *stratum granulosum* layers was most apparent after IMA-06504, IMA-07101, and IMA-08401 exposure (Figure 4A) and correlated to the levels of *CYP1A1* expression (Figure 4B). We also observed epidermal thickening and induction of *stratum corneum* layers most notably after AHR activation via TCDD and the TASQ derivatives. *FLG* protein expression levels were most strongly induced by TASQ derivative IMA-06504 and its prodrug IMA-07101 (Figure 4C). This finding was further substantiated by *loricrin* (*LOR*) and *involucrin* (*IVL*) immunostainings of IMA-07101 exposed HEEs (Supplemental Figure S2A), and subsequent semi-quantitative analysis (Supplemental Figures S2B and S3). Thus, activation of AHR signaling by LAQ and TASQ derivatives resulted in similar stimulating effects on epidermal development and formation as previously described for coal tar [7].

2.4. Therapeutic Effect of IMA-Compounds in Organotypic AD-like Epidermal Models

The potential of IMA-compounds to counteract detrimental effects of Th2 cytokines (e.g., IL-4) on epidermal differentiation protein expression, as seen for coal tar treatment, was investigated in an AD-like disease model. Hereto, HEEs generated from human primary keratinocytes harboring a heterozygous *FLG* mutation (Supplemental Table S2) were exposed to 10 ng/mL IL-4 for 96 h in total. After the first 24 h (disease initiation phase), the AD-HEEs were additionally stimulated with 1 nM of IMA-06504, IMA-07101, IMA-01403 (as a negative control) and TCDD for the final 72 h (treatment phase). IL-4 treated HEEs present with a thickened epidermis with fewer granular layers. Treatment with the TASQ derivatives increased the number of granular layers (Figure 5B). AHR activation in the AD-model by the TASQ derivatives and TCDD was verified by *CYP1A1* protein expression detection (Supplemental Figure S2A). The IL-4 mediated downregulation of *FLG*, *LOR*, and *IVL* expression, indicated by irregular staining patterns and staining of less epidermal layers, was effectively counteracted by IMA-07101 and its active metabolite IMA-06504. IMA-01403 was ineffective (Figure 5B). These findings were substantiated by semi-quantitative analysis (Supplemental Figure S2B).

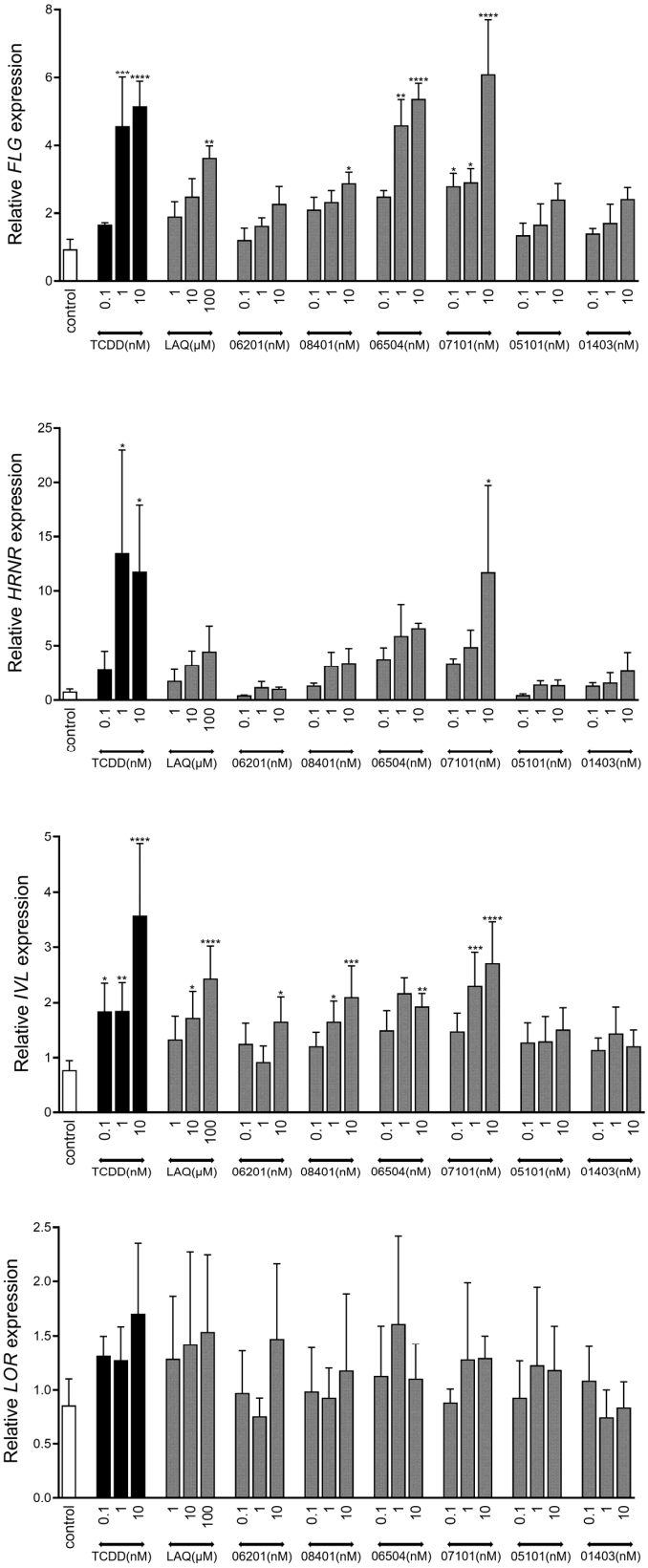

Figure 3. Upregulation of epidermal differentiation in vitro. Expression analysis of terminal differentiation genes *filaggrin* (*FLG*), *hornerin* (*HRNR*), *involucrin* (*IVL*), and *loricrin* (*LOR*) after 48 h stimulation (re-stimulation after 24 h) of monolayer primary human keratinocytes ($n = 3$) with a concentration series of the IMA-compounds, LAQ, and TCDD. * $p < 0.05$, ** $p < 0.01$, *** $p < 0.001$, **** $p < 0.0001$. Mean +/− SEM.

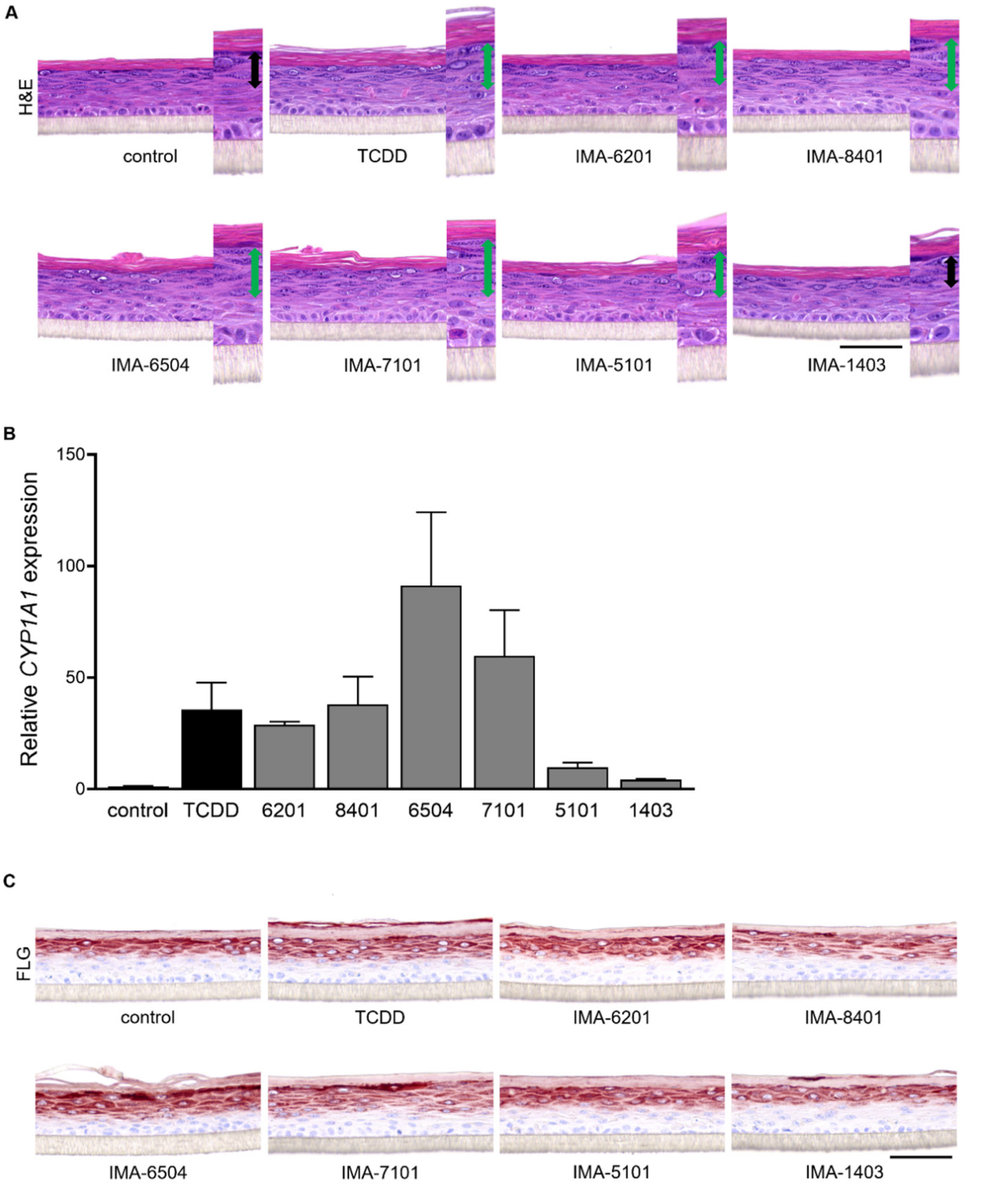

Figure 4. AHR activation and induction of epidermal differentiation in human epidermal equivalents. (**A**) H&E staining of human epidermal equivalents (HEEs) stimulated with 1 nM of IMA-compounds and TCDD for 96 h (re-stimulated after 48 h). Double headed arrows in magnified images indicate *stratum granulosum* layers (green arrows show an increase compared to the control-HEE). (**B**) *CYP1A1* mRNA levels ($n = 2$), mean +/− SEM. (**C**) Immunostaining for *filaggrin* (*FLG*) after 96 h of stimulation with IMA-compounds. Scale bar = 100 μm.

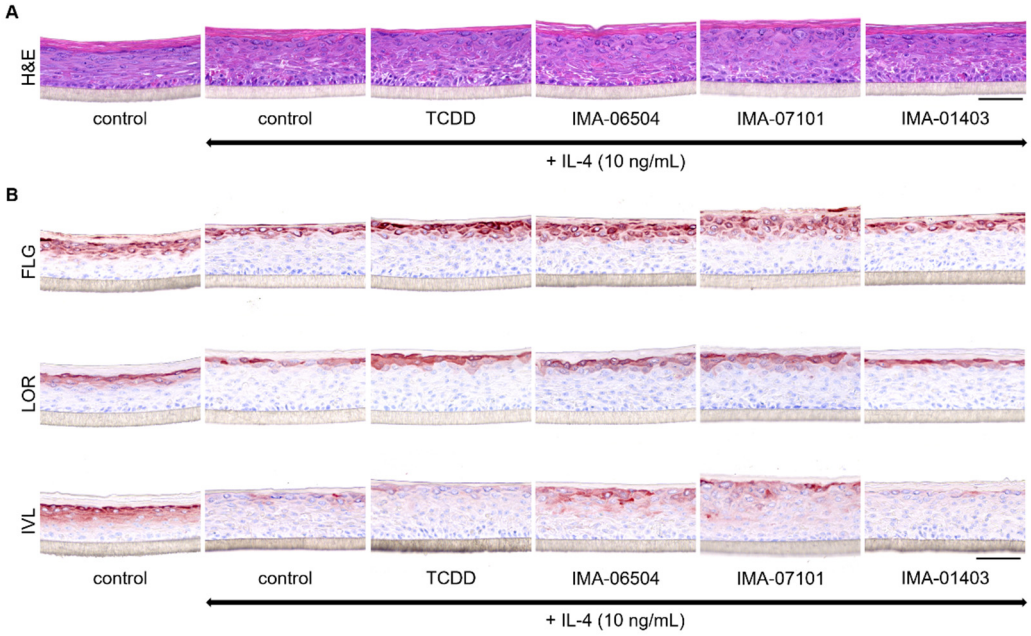

Figure 5. Therapeutic effect of TASQ derivatives in the AD-HEE model. (**A**) H&E staining of HEEs stimulated with 10 ng/mL IL-4 for 24 h followed by co-stimulation with the compounds for another 72 h. (**B**) Analysis of epidermal differentiation proteins via immunostainings for *filaggrin* (*FLG*), *loricrin* (*LOR*) and *involucrin* (*IVL*). Scale bar = 100 µm.

3. Discussion

In search of novel therapeutic AHR ligands for the treatment of inflammatory skin diseases, we here showed that carboxamide derivates are full AHR agonists in the low nanomolar range. TASQ metabolites most effectively induce *FLG* and other epidermal proteins important for skin barrier function, both in normal skin conditions and in a Th2-cytokine dominated inflammatory milieu representing AD-like inflammation.

The first compound from the carboxamide compound class, ROQ (drug name Linomide) was withdrawn from clinical trials due to severe drug-related adverse events in phase III trials with MS patients. [40–42]. Thereafter, LAQ and TASQ were developed and intended as safer derivatives [43,44]. Phase II/III clinical trials indicate therapeutic efficacy of LAQ in patients with multiple sclerosis [45,46], as also confirmed in recent meta-analysis [47]. Herein, a significantly higher risk of LAQ treatment was associated with back pain, headache, and vomiting [47]. Tasquinimod is intended for the oral treatment of prostate cancer, but also comes with adverse events (e.g., skeletal pain, digestive disorders, insomnia) [48,49]. Systemic exposure of exogenous AHR ligands may modulate and disrupt physiological AHR signaling given its expression in many tissues [22,50]. Topical application and thus local and tissue specific targeting in dermatological indications may therefore provide a better setting for the use of AHR ligands as therapeutics. Lead optimization of LAQ and TASQ resulted in increased potency of AHR activation in keratinocytes as LAQ only elevated AHR target gene levels at micromolar concentrations, whereas the IMA-metabolites induced AHR signaling already at 1 nM. This important step resulted in the first positive preclinical in vitro studies for dermatological indications herein described and provides solid ground for further preclinical development and topical formulation.

The in vivo safety aspects of the IMA-compounds have been studied in rodents, where no clinical signs of subacute toxicity were observed upon systemic exposure [36], other than generic AHR-mediated responses not relating to dioxin-induced toxicity. IMA-06201 and IMA-06504 were classified as non-mutagenic in in vitro analysis [35]. Furthermore, IMA-compounds are predicted to be faster metabolized to inactive compounds as compared to TCDD, which may be supportive of an improved safety profile [35,36]. Of note, TASQ derivatives were not rapidly metabolized and inactivated in keratinocyte monolayer

cultures, as indicated by the induced *AHRR* expression and *CYP1A1* enzyme activity after 48 h at similar levels as TCDD. These findings advocate for additional studies with prolonged culturing of keratinocytes after single dosing to determine the duration of AHR activation (e.g., *CYP1A1* expression dynamics) which may indicate TASQ metabolism rates and AHR ligand half-life as compared to dioxin. Our keratinocyte studies at least did not reveal cytotoxic effects (LDH leakage) or detrimental effects on the epidermal viability and morphology after exposure to IMA-compounds up to 96 h. However, also for TCDD, no acute cellular toxicity was observed, confirming the need for data on prolonged exposure to IMA-compounds, also including topical exposure in formulations rather than supplementation of culture medium as herein used.

The induction of epidermal differentiation by TASQ derivatives (even in the presence of IL-4) appeared more efficacious than for TCDD. This enables future dose reduction strategies for at least IMA-07101. Ideally, induction of epidermal differentiation should be retained while *CYP1A1* enzymatic levels are minimized. *CYP1A1* is associated with phase 1 metabolism and the generation of mutagenic epoxides from certain environmental pollutants. Although in vivo, CYP450 enzymes appear more important for detoxication than their activation of carcinogens [51]. Moreover, sustained *CYP1A1* activity may metabolize endogenous AHR ligands hence resulting in deprived physiological AHR signaling and skin tissue that is prone to inflammatory processes [51–53]. Besides concerns on phase 1 metabolism by *CYP1A1* due to AHR activation, a specific side effect, folliculitis, is reported in patients treated with topical AHR-activating therapies, such as coal tar and tapinarof [54,55]. The likelihood of other ligand classes, such as the IMA-compounds here investigated, causing similar side effects should be subject of further research.

TASQ derivatives IMA-06504 and IMA-07101 were most potent and effective for AHR-mediated induction of epidermal differentiation and the rescue of epidermal AD hallmarks by IL-4. The accelerated formation and development of the epidermis and skin barrier function upon AHR activation has also been shown upon in vivo TCDD treatment [10], in vitro coal tar treatment [7], and in Chinese traditional medicine [23]. Next to the regulation of terminal differentiation, AHR signaling was also reported to mediate keratinocyte proliferation [17,56]. Considering that proliferation and differentiation processes in both AD and Pso are disturbed, and that therapeutic effects of AHR activation are not specific to AD but are also demonstrated in Pso patients [57], efficacy of IMA-compounds in psoriasiform inflammation may be expected. Further preclinical studies are recommended including topical formulations and efficacy studies using other experimental AD models or ex vivo skin biopsies.

In future years, the search for novel or existing AHR-targeting drugs with high efficacies and minimized side effects will expand the currently limited arsenal of AHR-targeting therapeutics. Lead optimization of existing drug compounds, as we showed here for quinoline-3-carboxamide derivatives, is a promising strategy for the development of novel therapeutic AHR ligands to feed pharmaceutical pipelines.

4. Materials and Methods

4.1. Synthesis of IMA-Compounds

Synthetic preparations of LAQ and IMA-compounds, except for IMA-01403, are described in patent application WO2012/050500A1 [34]. IMA-01403 was prepared by benzylation of N-(2,4-dimethoxybenzyl)-N-phenyl-1,2-dihydro-4-hydroxy-1-methyl-2-oxo-quinoline-3-carboxamide [34] using BnBr (1,5 eq.) and K_2CO_3 (2 eq.) in DMF at 60 °C overnight, followed by concentration and conventional workup. The crude product was deprotected (cleavage of N-2,4-dimethoxybenzyl) using cerium ammonium nitrate (CAN, 3 eq., 0,1 M in 95% aq. MeCN) at room temperature for 20 min, followed by concentration conventional workup and purification by silica chromatography (CH_2Cl_2) to give IMA-01403 in 50% overall yield.

^{1}H NMR (400 MHz, $CDCl_3$) δ 3.75 (s, 3H), 5.45 (s, 2H), 7.14 (t, 1H), 7.25 (d, 1H), 7.32–7.47 (m, 8H), 7.65 (t, 1H), 7.77 (d, 2H), 8.09 (d, 1H), 10.71 (s, 1H).

4.2. HepG2 (40/6) Luciferase Reporter Assay

Human HepG2 (40/6) AHR reporter cells (hepatocellular carcinoma liver cells) were seeded in a 24-well format in Minimal Essential Medium Eagle (α-MEM, Sigma-Aldrich, St. Louis, MO, USA) supplemented with 1% penicillin/streptomycin and 8% fetal bovine serum (125.000 cells in 500 µL). After 24 h, cells were stimulated with LAQ (100, 10, or 1 µM), IMA-compounds (10, 1, 0.1, or 0.01 nM), and TCDD (10 nM) for 4 h at 37 °C with 5% CO_2. Thereafter, the cells were lysed in 200 mL lysis buffer (20 mM Tris-HCl, pH 7.8, 1% Triton X-100, 150 mM NaCl and 2 mM dithiothreitol) and stored at −80 °C. To detect luciferase activity, 20 µL cell lysate was mixed with 40 µL luciferase activity assay reagent (Promega Luciferase Assay system) and the luminescence signal measured (Synergy HT microplate reader, BioTek, Winooski, VT, USA).

4.3. Primary Keratinocyte Isolation

Surplus human skin was obtained from plastic surgery. Human primary keratinocytes were isolated as previously described and stored in liquid nitrogen (according to the principles of the Declaration of Helsinki) [58].

4.4. Monolayer Primary Keratinocyte Culture

Human primary keratinocytes were cultured submerged in 24-well plates at 37 °C with 5% CO_2 using keratinocyte growth medium with required growth factors and supplements (KGM, Lonza; without antibiotics) until confluency was reached [59]. Keratinocyte differentiation was initiated by depletion of growth factors and the cells were simultaneously stimulated with the IMA-compounds (10, 1, or 0.1 nM), TCDD (10, 1, or 0.1 nM), and LAQ (100, 10, or 1 µM). Keratinocytes were harvested after 48 h of stimulation (re-stimulated after 24 h) and processed for RNA isolation and subsequent qPCR analysis.

4.5. Lactate Dehydrogenase (LDH) Assay

The supernatant of the above-mentioned monolayer culture experiment was collected after 24 h of compound stimulation. Keratinocytes treated with 1% Triton X-100 in KGM were used as a positive control for 100% cell death. A cytotoxicity detection kit (Roche) was used to measure LDH activity according to the manufacturer's protocol and absorbance was read at 490 nm with a microplate reader (Bio-Rad).

4.6. CYP1A1 Enzyme Activity Assay

The P450-Glo™ *CYP1A1* assay system (Promega, Madison, WI, USA) was used to measure *CYP1A1* enzyme activity according to the manufacturer's protocol. Keratinocytes were treated as described previously (see monolayer primary keratinocyte culture). After 48 h of stimulation (refreshed after 24 h), cells were washed with PBS after which 200 µL Luc-CEE substrate solution in KGM without growth factors was added to the wells and incubated for 3 h at 37 °C with 5% CO_2. The culture medium was collected and mixed with luciferin detection reagent for detection of luminescence (Synergy HT microplate reader, BioTek, Winooski, VT, USA).

4.7. Human Epidermal Equivalent (HEE) Culture (Normal Skin and Atopic Dermatitis Model)

HEEs were generated according to the protocols previously described [58]. Briefly, 24-well cell culture inserts (ThinCert, Greiner Bio-One or Nunc, Thermo Fisher Scientific, Waltham, MA, USA) were coated with rat tail collagen (100 µg/mL, BD Biosciences, Franklin Lakes, NJ, USA) at 4 °C for 1 h. Then, 100.000–150.000 primary human keratinocytes were seeded submerged in 100–150 µL CnT-prime medium (CELLnTEC) After 48 h, cultures were switched to 3D differentiation medium, consisting of 60% CnT-Prime 3D Barrier medium (CELLnTEC) and 40% High Glucose Dulbecco's Modified Eagle's Medium (DMEM, Sigma-Aldrich, St. Louis, MO, USA). Then, 24 h later, the HEEs were lifted to the air–liquid interface (ALI), after which the differentiation medium was refreshed every other day.

In the normal skin model, HEEs were treated with the IMA-compounds (1 nM) and TCDD (1 nM) at day 4 of the ALI for 96 h (re-stimulation after 48 h). At day 8, HEEs were harvested and processed for qPCR and immunohistochemical analysis.

To generate an atopic dermatitis (AD)-like (AD-HEE) model [7,60–62], human primary $FLG^{+/-}$ keratinocytes (Supplemental Table S2) were used in combination with the disease-associated cytokine interleukin-4 (IL-4). AD-HEEs were first stimulated with IL-4 (10 ng/mL, Peprotech (supplemented with 0.05% bovine serum albumin, BSA, Sigma-Aldrich, St. Louis, MO, USA)) at day 4 of the ALI. After 24 h of disease initiation, HEEs were co-stimulated with the TASQ derivatives (IMA-06504 and IMA-07101), IMA-01403 and TCDD at a concentration of 1 nM and harvested 72 h later (re-stimulation after 48 h) for immunohistochemical analysis.

4.8. Immunohistochemistry

HEEs were fixed in 4% formalin for 4 h and processed for routine histology. The 6 µm paraffin sections were stained with hematoxylin and eosin (Sigma-Aldrich, St. Louis, MO, USA) after deparaffinization. For immunohistochemical analysis, sections were stained using an indirect immunoperoxidase technique with avidin–biotin complex enhancement (Vectastain, Vector Laboratories) using antibodies listed in Supplemental Table S3.

4.9. RNA Isolation Real-Time Quantitative PCR (RT-qPCR)

RNA was isolated with the Tissue Total RNA Kit (Favorgen, Vienna, Austria) according to the manufacturer's protocol. RNA was treated with DNAseI (Invitrogen, Waltham, MA, USA) and used for cDNA synthesis using SuperScript IV VILO Master Mix (Invitrogen, Waltham, MA, USA) according to the manufacturer's protocol. RT-qPCR analysis was performed using SYBR Green (Bio-Rad, Hercules, CA, USA). Target gene expression was normalized to the expression of the house keeping gene human acidic ribosomal phosphoprotein P0 (RPLP0) and relative expression levels were calculated by the ΔΔCt method [63]. Primer sequences (Biolegio, Nijmegen, The Netherlands) are depicted in Supplemental Table S4.

4.10. Quantification of Differentiation Protein Expression in HEEs

Image acquisition of HEE immunostainings was performed by a ZEISS Axio Imager equipped with a ZEISS Axiocam 105 color Digital Camera and a 40× objective. The ZEISS Axiocam 105 color is a compact 5-megapixel camera (2560 × 1920 pixels) for high resolution images with a 1/2.5" sensor. Two images per slide were chosen as representative for the whole culture and stored in CZI format. The images were analyzed with the cell image analysis software CellProfiler (Broad Institute) [64]. Software pipelines for *filaggrin* (*FLG*), *loricrin* (*LOR*), and *involucrin* (*IVL*) analysis were created (available upon request) and GraphPad Prism 9.0 was used for the visualization of the data. The quantified data is shown as the protein area occupied (μm^2) per millimeter length of the epidermis. Because this value does not normalize for the thickness of the epidermis (differences in epidermal thickness were observed after compound stimulation), we also calculated the area of expression as percentage of the epidermal surface for comparison.

4.11. Statistics

Statistical analyses were performed using GraphPad Prism 9.0 on experiments of at least $n = 3$ replicates. To determine statistical significance between multiple groups for the in vitro monolayer cultures, paired one-way analysis of variance (ANOVA; mixed effects model for repeated measures data (one missing value)) was performed followed by Tukey's multiple comparison post hoc test. For the data obtained by CellProfiler software, the calculated protein area (μm^2) per millimeter length was used to analyze significant differences between multiple groups by performing the Friedman test (paired nonparametric test), indicated as (p = x.xx) in the legend. If significant, Dunn's multiple

comparison post hoc test was executed. Each culture experiment (monolayer or organotypic HEE) includes biological donor replicates.

Supplementary Materials: The following supporting information can be downloaded at: https://www.mdpi.com/article/10.3390/ijms23031773/s1.

Author Contributions: Conceptualization, L.P. and E.H.v.d.B.; data curation, G.R.; formal analysis, G.R.; funding acquisition, E.H.v.d.B.; investigation, G.R., N.J.M.v.d.B. and I.M.J.J.v.V.-W.; methodology, G.R.; project administration, E.H.v.d.B.; resources, L.P. and E.H.v.d.B.; software, P.E.J.v.E.; supervision, J.P.H.S. and E.H.v.d.B.; validation, G.R.; visualization, G.R.; writing—original draft, G.R., N.J.M.v.d.B., L.P. and J.P.H.S.; writing—review and editing, G.R., L.P., J.P.H.S. and E.H.v.d.B. All authors have read and agreed to the published version of the manuscript.

Funding: This investigator-initiated study is funded by research grants from Radboud Institute of Molecular Life Sciences, National Institute of Health (NIH, grant ES028244). The funders had no role in study design, data collection and analysis, decision to publish, or preparation of the manuscript.

Institutional Review Board Statement: Not applicable.

Informed Consent Statement: Not applicable.

Data Availability Statement: The datasets used and analyzed during the current study are available from the corresponding author (E.H.v.d.B.) upon request.

Acknowledgments: We thank Nando Katoele and Denica Daniel for providing technical support during experiments.

Conflicts of Interest: The authors declare no conflict of interest.

Abbreviations

FLG	filaggrin
AD	atopic dermatitis
Pso	psoriasis
AHR	aryl hydrocarbon receptor
CYP1A1	cytochrome P450 1A1
TCDD	2,3,7,8-tetrachlorodibenzodioxin
LAQ	laquinimod
TASQ	tasquinimod
ROQ	roquinimex
IMA	immunahr
IL-4	interleukin-4
HEE	human epidermal equivalent

References

1. Palmer, C.N.; Irvine, A.D.; Terron-Kwiatkowski, A.; Zhao, Y.; Liao, H.; Lee, S.P.; Goudie, D.R.; Sandilands, A.; Campbell, L.E.; Smith, F.J.; et al. Common loss-of-function variants of the epidermal barrier protein filaggrin are a major predisposing factor for atopic dermatitis. *Nat. Genet.* **2006**, *38*, 441–446. [CrossRef] [PubMed]
2. Sandilands, A.; Terron-Kwiatkowski, A.; Hull, P.R.; O'Regan, G.M.; Clayton, T.H.; Watson, R.M.; Carrick, T.; Evans, A.T.; Liao, H.; Zhao, Y.; et al. Comprehensive analysis of the gene encoding filaggrin uncovers prevalent and rare mutations in ichthyosis vulgaris and atopic eczema. *Nat. Genet.* **2007**, *39*, 650–654. [CrossRef] [PubMed]
3. Brown, S.J.; Kroboth, K.; Sandilands, A.; Campbell, L.E.; Pohler, E.; Kezic, S.; Cordell, H.J.; McLean, W.H.; Irvine, A.D. Intragenic copy number variation within filaggrin contributes to the risk of atopic dermatitis with a dose-dependent effect. *J. Invest. Dermatol.* **2012**, *132*, 98–104. [CrossRef]
4. Knuppel, S.; Esparza-Gordillo, J.; Marenholz, I.; Holzhutter, H.G.; Bauerfeind, A.; Ruether, A.; Weidinger, S.; Lee, Y.A.; Rohde, K. Multi-locus stepwise regression: A haplotype-based algorithm for finding genetic associations applied to atopic dermatitis. *BMC Med. Genet.* **2012**, *13*, 8. [CrossRef] [PubMed]
5. Trzeciak, M.; Wesserling, M.; Bandurski, T.; Glen, J.; Nowicki, R.; Pawelczyk, T. Association of a Single Nucleotide Polymorphism in a Late Cornified Envelope-like Proline-rich 1 Gene (LELP1) with Atopic Dermatitis. *Acta Derm. Venereol.* **2016**, *96*, 459–463. [CrossRef]

6. Marenholz, I.; Rivera, V.A.; Esparza-Gordillo, J.; Bauerfeind, A.; Lee-Kirsch, M.A.; Ciechanowicz, A.; Kurek, M.; Piskackova, T.; Macek, M.; Lee, Y.A. Association screening in the Epidermal Differentiation Complex (EDC) identifies an SPRR3 repeat number variant as a risk factor for eczema. *J. Invest. Dermatol.* **2011**, *131*, 1644–1649. [CrossRef]
7. van den Bogaard, E.H.; Bergboer, J.G.; Vonk-Bergers, M.; van Vlijmen-Willems, I.M.; Hato, S.V.; van der Valk, P.G.; Schroder, J.M.; Joosten, I.; Zeeuwen, P.L.; Schalkwijk, J. Coal tar induces AHR-dependent skin barrier repair in atopic dermatitis. *J. Clin. Invest.* **2013**, *123*, 917–927. [CrossRef]
8. Smits, J.P.H.; Ederveen, T.H.A.; Rikken, G.; van den Brink, N.J.M.; van Vlijmen-Willems, I.; Boekhorst, J.; Kamsteeg, M.; Schalkwijk, J.; van Hijum, S.; Zeeuwen, P.; et al. Targeting the Cutaneous Microbiota in Atopic Dermatitis by Coal Tar via AHR-Dependent Induction of Antimicrobial Peptides. *J. Invest. Dermatol.* **2020**, *140*, 415–424.e410. [CrossRef]
9. Loertscher, J.A.; Sattler, C.A.; Allen-Hoffmann, B.L. 2,3,7,8-Tetrachlorodibenzo-p-dioxin alters the differentiation pattern of human keratinocytes in organotypic culture. *Toxicol. Appl. Pharmacol.* **2001**, *175*, 121–129. [CrossRef]
10. Sutter, C.H.; Bodreddigari, S.; Campion, C.; Wible, R.S.; Sutter, T.R. 2,3,7,8-Tetrachlorodibenzo-p-dioxin increases the expression of genes in the human epidermal differentiation complex and accelerates epidermal barrier formation. *Toxicol. Sci.* **2011**, *124*, 128–137. [CrossRef]
11. Fritsche, E.; Schafer, C.; Calles, C.; Bernsmann, T.; Bernshausen, T.; Wurm, M.; Hubenthal, U.; Cline, J.E.; Hajimiragha, H.; Schroeder, P.; et al. Lightening up the UV response by identification of the arylhydrocarbon receptor as a cytoplasmatic target for ultraviolet B radiation. *Proc. Natl. Acad. Sci. USA* **2007**, *104*, 8851–8856. [CrossRef] [PubMed]
12. Jin, U.H.; Lee, S.O.; Sridharan, G.; Lee, K.; Davidson, L.A.; Jayaraman, A.; Chapkin, R.S.; Alaniz, R.; Safe, S. Microbiome-derived tryptophan metabolites and their aryl hydrocarbon receptor-dependent agonist and antagonist activities. *Mol. Pharmacol.* **2014**, *85*, 777–788. [CrossRef] [PubMed]
13. Tan, Y.Q.; Chiu-Leung, L.C.; Lin, S.M.; Leung, L.K. The citrus flavonone hesperetin attenuates the nuclear translocation of aryl hydrocarbon receptor. *Comp. Biochem. Physiol. C Toxicol. Pharmacol.* **2018**, *210*, 57–64. [CrossRef] [PubMed]
14. Uberoi, A.; Bartow-McKenney, C.; Zheng, Q.; Flowers, L.; Campbell, A.; Knight, S.A.B.; Chan, N.; Wei, M.; Lovins, V.; Bugayev, J.; et al. Commensal microbiota regulates skin barrier function and repair via signaling through the aryl hydrocarbon receptor. *Cell. Host Microbe* **2021**, *29*, 1235–1248.e1238. [CrossRef] [PubMed]
15. van den Bogaard, E.H.; Esser, C.; Perdew, G.H. The aryl hydrocarbon receptor at the forefront of host-microbe interactions in the skin: A perspective on current knowledge gaps and directions for future research and therapeutic applications. *Exp. Dermatol.* **2021**, *30*, 1477–1483. [CrossRef]
16. Gialitakis, M.; Tolaini, M.; Li, Y.; Pardo, M.; Yu, L.; Toribio, A.; Choudhary, J.S.; Niakan, K.; Papayannopoulos, V.; Stockinger, B. Activation of the Aryl Hydrocarbon Receptor Interferes with Early Embryonic Development. *Stem Cell Rep.* **2017**, *9*, 1377–1386. [CrossRef]
17. van den Bogaard, E.H.; Podolsky, M.A.; Smits, J.P.; Cui, X.; John, C.; Gowda, K.; Desai, D.; Amin, S.G.; Schalkwijk, J.; Perdew, G.H.; et al. Genetic and pharmacological analysis identifies a physiological role for the AHR in epidermal differentiation. *J. Invest. Dermatol.* **2015**, *135*, 1320–1328. [CrossRef]
18. Haas, K.; Weighardt, H.; Deenen, R.; Kohrer, K.; Clausen, B.; Zahner, S.; Boukamp, P.; Bloch, W.; Krutmann, J.; Esser, C. Aryl Hydrocarbon Receptor in Keratinocytes Is Essential for Murine Skin Barrier Integrity. *J. Invest. Dermatol.* **2016**, *136*, 2260–2269. [CrossRef]
19. Gutierrez-Vazquez, C.; Quintana, F.J. Regulation of the Immune Response by the Aryl Hydrocarbon Receptor. *Immunity* **2018**, *48*, 19–33. [CrossRef]
20. Roman, A.C.; Carvajal-Gonzalez, J.M.; Rico-Leo, E.M.; Fernandez-Salguero, P.M. Dioxin receptor deficiency impairs angiogenesis by a mechanism involving VEGF-A depletion in the endothelium and transforming growth factor-beta overexpression in the stroma. *J. Biol. Chem.* **2009**, *284*, 25135–25148. [CrossRef]
21. Kimura, E.; Kubo, K.I.; Endo, T.; Nakajima, K.; Kakeyama, M.; Tohyama, C. Excessive activation of AhR signaling disrupts neuronal migration in the hippocampal CA1 region in the developing mouse. *J. Toxicol. Sci.* **2017**, *42*, 25–30. [CrossRef] [PubMed]
22. Zhang, N. The role of endogenous aryl hydrocarbon receptor signaling in cardiovascular physiology. *J. Cardiovasc. Dis. Res.* **2011**, *2*, 91–95. [CrossRef] [PubMed]
23. Furue, M.; Takahara, M.; Nakahara, T.; Uchi, H. Role of AhR/ARNT system in skin homeostasis. *Arch. Dermatol. Res.* **2014**, *306*, 769–779. [CrossRef] [PubMed]
24. Quintana, F.J.; Sherr, D.H. Aryl hydrocarbon receptor control of adaptive immunity. *Pharmacol. Rev.* **2013**, *65*, 1148–1161. [CrossRef]
25. Haarmann-Stemmann, T.; Esser, C.; Krutmann, J. The Janus-Faced Role of Aryl Hydrocarbon Receptor Signaling in the Skin: Consequences for Prevention and Treatment of Skin Disorders. *J. Invest. Dermatol.* **2015**, *135*, 2572–2576. [CrossRef]
26. Denison, M.S.; Soshilov, A.A.; He, G.; DeGroot, D.E.; Zhao, B. Exactly the same but different: Promiscuity and diversity in the molecular mechanisms of action of the aryl hydrocarbon (dioxin) receptor. *Toxicol. Sci.* **2011**, *124*, 1–22. [CrossRef]
27. Smith, S.H.; Jayawickreme, C.; Rickard, D.J.; Nicodeme, E.; Bui, T.; Simmons, C.; Coquery, C.M.; Neil, J.; Pryor, W.M.; Mayhew, D.; et al. Tapinarof Is a Natural AhR Agonist that Resolves Skin Inflammation in Mice and Humans. *J. Invest. Dermatol.* **2017**, *137*, 2110–2119. [CrossRef] [PubMed]

28. Peppers, J.; Paller, A.S.; Maeda-Chubachi, T.; Wu, S.; Robbins, K.; Gallagher, K.; Kraus, J.E. A phase 2, randomized dose-finding study of tapinarof (GSK2894512 cream) for the treatment of atopic dermatitis. *J. Am. Acad. Dermatol.* **2019**, *80*, 89–98.e83. [CrossRef]
29. Boros, F.; Vecsei, L. Progress in the development of kynurenine and quinoline-3-carboxamide-derived drugs. *Expert. Opin. Investig. Drugs* **2020**, *29*, 1223–1247. [CrossRef]
30. Kaye, J.; Piryatinsky, V.; Birnberg, T.; Hingaly, T.; Raymond, E.; Kashi, R.; Amit-Romach, E.; Caballero, I.S.; Towfic, F.; Ator, M.A.; et al. Laquinimod arrests experimental autoimmune encephalomyelitis by activating the aryl hydrocarbon receptor. *Proc. Natl. Acad. Sci. USA* **2016**, *113*, E6145–E6152. [CrossRef]
31. Wegner, C.; Stadelmann, C.; Pfortner, R.; Raymond, E.; Feigelson, S.; Alon, R.; Timan, B.; Hayardeny, L.; Bruck, W. Laquinimod interferes with migratory capacity of T cells and reduces IL-17 levels, inflammatory demyelination and acute axonal damage in mice with experimental autoimmune encephalomyelitis. *J. Neuroimmunol.* **2010**, *227*, 133–143. [CrossRef]
32. Bruck, W.; Wegner, C. Insight into the mechanism of laquinimod action. *J. Neurol. Sci.* **2011**, *306*, 173–179. [CrossRef] [PubMed]
33. Nilsson, B. New use of quinoline-3-carboxamide compounds. WO 95/24196A1, 8 March 1995.
34. Pettersson, L. 1,2-dihydro-4-hydroxy-2-oxo-quinoline-3-carboxanilides as AHR activators. WO 2012/050500, 19 April 2012.
35. Mahiout, S.; Tagliabue, S.G.; Nasri, A.; Omoruyi, I.M.; Pettersson, L.; Bonati, L.; Pohjanvirta, R. In vitro toxicity and in silico docking analysis of two novel selective AH-receptor modulators. *Toxicol. In Vitro* **2018**, *52*, 178–188. [CrossRef] [PubMed]
36. Mahiout, S.; Linden, J.; Esteban, J.; Sanchez-Perez, I.; Sankari, S.; Pettersson, L.; Hakansson, H.; Pohjanvirta, R. Toxicological characterisation of two novel selective aryl hydrocarbon receptor modulators in Sprague-Dawley rats. *Toxicol. Appl. Pharmacol.* **2017**, *326*, 54–65. [CrossRef] [PubMed]
37. Long, W.P.; Pray-Grant, M.; Tsai, J.C.; Perdew, G.H. Protein kinase C activity is required for aryl hydrocarbon receptor pathway-mediated signal transduction. *Mol. Pharmacol.* **1998**, *53*, 691–700. [CrossRef]
38. Kennedy, L.H.; Sutter, C.H.; Leon Carrion, S.; Tran, Q.T.; Bodreddigari, S.; Kensicki, E.; Mohney, R.P.; Sutter, T.R. 2,3,7,8-Tetrachlorodibenzo-p-dioxin-mediated production of reactive oxygen species is an essential step in the mechanism of action to accelerate human keratinocyte differentiation. *Toxicol. Sci.* **2013**, *132*, 235–249. [CrossRef]
39. Vu, Y.H.; Hashimoto-Hachiya, A.; Takemura, M.; Yumine, A.; Mitamura, Y.; Nakahara, T.; Furue, M.; Tsuji, G. IL-24 Negatively Regulates Keratinocyte Differentiation Induced by Tapinarof, an Aryl Hydrocarbon Receptor Modulator: Implication in the Treatment of Atopic Dermatitis. *Int. J. Mol. Sci.* **2020**, *21*, 9412. [CrossRef]
40. de Wit, R.; Pawinsky, A.; Stoter, G.; van Oosterom, A.T.; Fossa, S.D.; Paridaens, R.; Svedberg, A.; de Mulder, P.H. EORTC phase II study of daily oral linomide in metastatic renal cell carcinoma patients with good prognostic factors. *Eur. J. Cancer* **1997**, *33*, 493–495. [CrossRef]
41. Mackean, M.J.; Kerr, D.; Lesko, M.; Svedberg, A.; Hansson, F.; Jodrell, D.; Cassidy, J. A feasibility study of roquinimex (Linomide) and alpha interferon in patients with advanced malignant melanoma or renal carcinoma. *Br. J. Cancer* **1998**, *78*, 1620–1623. [CrossRef]
42. Noseworthy, J.H.; Wolinsky, J.S.; Lublin, F.D.; Whitaker, J.N.; Linde, A.; Gjorstrup, P.; Sullivan, H.C. Linomide in relapsing and secondary progressive MS: Part I: Trial design and clinical results. North American Linomide Investigators. *Neurology* **2000**, *54*, 1726–1733. [CrossRef]
43. Jonsson, S.; Andersson, G.; Fex, T.; Fristedt, T.; Hedlund, G.; Jansson, K.; Abramo, L.; Fritzson, I.; Pekarski, O.; Runstrom, A.; et al. Synthesis and biological evaluation of new 1,2-dihydro-4-hydroxy-2-oxo-3-quinolinecarboxamides for treatment of autoimmune disorders: Structure-activity relationship. *J. Med. Chem.* **2004**, *47*, 2075–2088. [CrossRef] [PubMed]
44. Isaacs, J.T.; Pili, R.; Qian, D.Z.; Dalrymple, S.L.; Garrison, J.B.; Kyprianou, N.; Bjork, A.; Olsson, A.; Leanderson, T. Identification of ABR-215050 as lead second generation quinoline-3-carboxamide anti-angiogenic agent for the treatment of prostate cancer. *Prostate* **2006**, *66*, 1768–1778. [CrossRef] [PubMed]
45. Haggiag, S.; Ruggieri, S.; Gasperini, C. Efficacy and safety of laquinimod in multiple sclerosis: Current status. *Ther. Adv. Neurol. Disord.* **2013**, *6*, 343–352. [CrossRef] [PubMed]
46. Polman, C.; Barkhof, F.; Sandberg-Wollheim, M.; Linde, A.; Nordle, O.; Nederman, T.; Laquinimod in Relapsing, M.S.S.G. Treatment with laquinimod reduces development of active MRI lesions in relapsing MS. *Neurology* **2005**, *64*, 987–991. [CrossRef]
47. Rouhi, F.; Mohammadpour, Z.; Noureini, S.K.; Abbastabar, H.; Harirchian, M.H.; Bitarafan, S. The effects and side effects of laquinimod for the treatment of multiple sclerosis patients: A systematic review and meta-analysis of clinical trials. *Eur. J. Clin. Pharmacol.* **2020**, *76*, 611–622. [CrossRef]
48. Gong, P.; Liu, H.; Liu, X.; Zhou, G.; Liu, M.; Yang, X.; Xiong, W.; Wang, Q.; Ma, J.; Ren, Z.; et al. Efficacy of tasquinimod in men with metastatic castration-resistant prostate cancer: A meta-analysis of randomized controlled trials. *Medicine* **2018**, *97*, e13204. [CrossRef]
49. Williamson, S.C.; Hartley, A.E.; Heer, R. A review of tasquinimod in the treatment of advanced prostate cancer. *Drug Des. Devel. Ther.* **2013**, *7*, 167–174. [CrossRef]
50. Bock, K.W. From TCDD-mediated toxicity to searches of physiologic AHR functions. *Biochem. Pharmacol.* **2018**, *155*, 419–424. [CrossRef]
51. Androutsopoulos, V.P.; Tsatsakis, A.M.; Spandidos, D.A. Cytochrome P450 CYP1A1: Wider roles in cancer progression and prevention. *BMC Cancer* **2009**, *9*, 187. [CrossRef]

52. Kyoreva, M.; Li, Y.; Hoosenally, M.; Hardman-Smart, J.; Morrison, K.; Tosi, I.; Tolaini, M.; Barinaga, G.; Stockinger, B.; Mrowietz, U.; et al. CYP1A1 Enzymatic Activity Influences Skin Inflammation Via Regulation of the AHR Pathway. *J. Invest. Dermatol.* **2021**, *141*, 1553–1563.e1553. [CrossRef]
53. van den Bogaard, E.H.; Perdew, G.H. The Enigma of AHR Activation in the Skin: Interplay among Ligands, Metabolism, and Bioavailability. *J. Invest. Dermatol.* **2021**, *141*, 1385–1388. [CrossRef] [PubMed]
54. Bissonnette, R.; Stein Gold, L.; Rubenstein, D.S.; Tallman, A.M.; Armstrong, A. Tapinarof in the treatment of psoriasis: A review of the unique mechanism of action of a novel therapeutic aryl hydrocarbon receptor-modulating agent. *J. Am. Acad. Dermatol.* **2021**, *84*, 1059–1067. [CrossRef] [PubMed]
55. Konstantinou, M.P.; Jendoubi, F.; Hegazy, S.; Bouznad, A.; Tauber, M.; Bulai-Livideanu, C.; Paul, C. Tapinarof-induced folliculitis: The paradigm of activation of the aryl hydrocarbon signaling pathway. *J. Am. Acad. Dermatol.* **2021**, *85*, e37–e38. [CrossRef]
56. Kalmes, M.; Hennen, J.; Clemens, J.; Blomeke, B. Impact of aryl hydrocarbon receptor (AhR) knockdown on cell cycle progression in human HaCaT keratinocytes. *Biol. Chem.* **2011**, *392*, 643–651. [CrossRef] [PubMed]
57. Lebwohl, M.G.; Gold, L.S.; Strober, B.; Papp, K.A.; Armstrong, A.W.; Bagel, J.; Kircik, L.; Ehst, B.; Hong, H.C.; Soung, J.; et al. Phase 3 trials of tapinarof cream for plaque psoriasis. *N. Engl. J. Med.* **2021**, *385*, 2219–2229. [CrossRef] [PubMed]
58. Rikken, G.; Niehues, H.; van den Bogaard, E.H. Organotypic 3D Skin Models: Human Epidermal Equivalent Cultures from Primary Keratinocytes and Immortalized Keratinocyte Cell Lines. *Methods Mol. Biol.* **2020**, *2154*, 45–61. [CrossRef]
59. Nygaard, U.H.; Niehues, H.; Rikken, G.; Rodijk-Olthuis, D.; Schalkwijk, J.; van den Bogaard, E.H. Antibiotics in cell culture: Friend or foe? Suppression of keratinocyte growth and differentiation in monolayer cultures and 3D skin models. *Exp. Dermatol.* **2015**, *24*, 964–965. [CrossRef]
60. Kamsteeg, M.; Bergers, M.; de Boer, R.; Zeeuwen, P.L.; Hato, S.V.; Schalkwijk, J.; Tjabringa, G.S. Type 2 helper T-cell cytokines induce morphologic and molecular characteristics of atopic dermatitis in human skin equivalent. *Am. J. Pathol.* **2011**, *178*, 2091–2099. [CrossRef]
61. Niehues, H.; Schalkwijk, J.; van Vlijmen-Willems, I.; Rodijk-Olthuis, D.; van Rossum, M.M.; Wladykowski, E.; Brandner, J.M.; van den Bogaard, E.H.J.; Zeeuwen, P. Epidermal equivalents of filaggrin null keratinocytes do not show impaired skin barrier function. *J. Allergy Clin. Immunol.* **2017**, *139*, 1979–1981.e1913. [CrossRef]
62. Niehues, H.; Rikken, G.; van Vlijmen-Willems, I.M.J.J.; Rodijk-Olthuis, D.; van Erp, P.E.J.; Zeeuwen, P.L.J.M.; Schalkwijk, J.; van den Bogaard, E.H. Identification of Keratinocyte Mitogens: Implications for Hyperproliferation in Psoriasis and Atopic Dermatitis. *JID Innov.* **2022**, *2*, 100066. [CrossRef]
63. Livak, K.J.; Schmittgen, T.D. Analysis of relative gene expression data using real-time quantitative PCR and the 2(-Delta Delta C(T)) Method. *Methods* **2001**, *25*, 402–408. [CrossRef] [PubMed]
64. McQuin, C.; Goodman, A.; Chernyshev, V.; Kamentsky, L.; Cimini, B.A.; Karhohs, K.W.; Doan, M.; Ding, L.; Rafelski, S.M.; Thirstrup, D.; et al. CellProfiler 3.0: Next-generation image processing for biology. *PLoS Biol.* **2018**, *16*, e2005970. [CrossRef] [PubMed]